Hydrol. Earth Syst. Sci. Discuss., 12, 609–637, 2015
www.hydrol-earth-syst-sci-discuss.net/12/609/2015/
doi:10.5194/hessd-12-609-2015

Hydrology and Earth System Sciences
Open Access
Discussions

A conceptual, distributed snow redistribution model

S. Frey and H. Holzmann

Institute of Water Management, Hydrology and Hydraulic Engineering, University of Natural Resources and Life Sciences, Vienna, Austria

Received: 10 December 2014 – Accepted: 22 December 2014 – Published: 14 January 2015

Correspondence to: S. Frey (simon.frey@boku.ac.at)

Published by Copernicus Publications on behalf of the European Geosciences Union.

Abstract

When applying conceptual hydrological models using a temperature index approach for snowmelt to high alpine areas often accumulation of snow during several years can be observed. Some of the reasons why these "snow towers" do not exist in nature are vertical and lateral transport processes. While snow transport models have been developed using grid cell sizes of tens to hundreds of square meters and have been applied in several catchments, no model exists using coarser cell sizes of one km^2. In this paper we present an approach that uses only gravity and snow density as a proxy for the age of the snow cover and land-use information to redistribute snow in the catchment of Ötztaler Ache, Austria. This transport model is implemented in the distributed rainfall–runoff model COSERO and a comparison between the standard model without using snow transport and the updated version is done using runoff and MODIS data for model validation. While the signal of snow redistribution can hardly be seen in the binary classification compared with MODIS, snow accumulation over several years can be prevented. In a seven year period the classic model would lead to snow accumulation of approximately 2900 mm SWE in high elevated regions whereas the updated version of the model does not show accumulation and does also predict discharge more precisely leading to a Kling–Gupta-Efficiency of 0.93 instead of 0.9.

1 Introduction

Conceptual models are widely used in hydrology. Examples are the HBV model (Bergström, 1976), PDM (Moore, 2007), GSM-SOCONT (Schaefli et al., 2005) or VIC (Wood et al., 1992) just to name a few. Many of these conceptual models use a temperature index approach to model snow melt and snow accumulation and even in some physically based models as e. g. versions of the SHE model (Bøggild et al., 1999) this method can be found. This approach has the advantage of being quite simple since it uses only temperature as input to determine whether precipitation occurs in the form of snow or rain and whether snow can be melted or not. A typical example of a temperature index method for snow modelling is the day degree approach (see for example Hock, 2003). A disadvantage is that snow accumulates as long as the air temperature does not rise above a certain threshold (often 0 °C) regardless of any other processes that may lead to snow melt like radiation or humidity. In high mountainous areas this may be the case for most days in the year leading to an intensive accumulation of snow in these areas. Many studies have tried to solve this problem.

Often wind speed and -direction are used to model snow drift (e.g. Bernhardt et al., 2009, 2010; Shulski and Seeley, 2004; Winstral et al., 2002; Liston and Sturm, 1998). Also the physical based SNOWPACK model (Bartelt and Lehning, 2002) used in avalanche research uses wind to determine redistribution of snow. Unfortunately, wind fields are afflicted with errors, especially if generated by regional circulation models (RCM) for climate change scenario studies (Nikulin et al., 2011). Furthermore, these models need spatial information on a small scale of grid cells of only 100s to 1000s of square meters. However, the difficulties of snow accumulation also occur when models with coarser cell sizes are used. To our knowledge, no model for redistributing snow on a 1 km × 1 km grid size exists. In this paper we present a simple approach to deal with snow in high mountainous regions and its application in the catchment of Ötztaler Ache in Tyrol, Austria.

2 Theoretical background of snow transport processes

Snow depths vary greatly even on high-resolution scales (e. g. Helfricht et al., 2014). During the accumulation period, according to Liston (2004), primarily three mechanisms are responsible for these variations: (a) snow-canopy interactions in forest covered regions, (b) wind induced snow redistribution and (c) orographic influences on snow fall. These mechanisms influence snow patterns on different spatial scales.

HESSD
12, 609–637, 2015

Differences in tree species like evergreen gymnosperms or clear deciduous trees as well as the density of the canopy layer cause spatial variability of the snow layer (Garvelmann et al., 2013; Liston, 2004; Pomeroy et al., 2002).

Besides the impact of vegetation, wind is the most dominant factor influencing snow patterns in alpine terrain. Snow is transported from exposed ridges to the lee side of these ridges, valleys and vegetation covered areas (Essery et al., 1999; Liston and Sturm, 1998). One has to be aware, that besides of the physical transport of solid snow wind also stimulates sublimation processes (e. g. Liston and Sturm, 1998).

The third mechanism influences snow patterns on a larger scale of one to several kilometres (e. g. Barros and Lettenmaier, 1994). Non-uniform snow distributions are caused by interactions of the atmosphere (air pressure, humidity, atmospheric stability) with topography (Liston, 2004).

During the ablation period, spatial snow distributions are mainly influenced by differences snow melt behaviours. On the Northern Hemisphere snowmelt from south-facing slopes is generally higher than snowmelt on north-facing slopes due to the inclination of radiation. Also vegetation influences melting behaviours. Shading reduces snowmelt whereas emitted long wave radiation increases it (Garvelmann et al., 2013; Pohl et al., 2014).

3 Model description

3.1 Hydrological model COSERO

COSERO is a spatially distributed conceptual hydrological model which is similar to the HBV model (Bergström, 1976). Originally developed for modelling discharge of the Austrian rivers Enns and Steyer (Nachtnebel et al., 1993), it has recently been used for different purposes like climate change studies (e. g. Kling et al., 2012, 2014b; Stanzel and Nachtnebel, 2010), investigating the role of evapotranspiration in high alpine regions (Herrnegger et al., 2012) and operational runoff forecasting (Stanzel et al., 2008). Po-

HESSD
12, 609–637, 2015

tential evapotranspiration is calculated using the Thornthwaite method (Thornthwaite, 1948). Discharge due to rainfall and snow-/ice melt is estimated using the same non-linear function of soil moisture as the original HBV. In this study, the model is run using daily time steps however it is capable of using hourly or monthly time steps. In the latter case, intra-monthly variations are considered for snow and interception processes as well as for soil moisture (Kling et al., 2014a). A schematic overview of the model is given by Fig. 1 and a detailed description of the model can be found in Kling et al. (2014a), where the model was applied to several catchments across Europe, Africa and Australia. In this study, snow parameters were not calibrated and therefore the snow module is not fully explained in detail. This will be done in the following. Equations (1) to (7) were taken from the original model by Stanzel and Nachtnebel (2010), all other methods were developed in this study.

Numerous studies have shown that sub-grid variability of snow depths can be described by a two parameter log-normal distribution (e. g. Donald et al., 1995; Pomeroy et al., 1998). This distribution can be interpreted as a description of small scale snow distribution processes. COSERO uses five snow classes per cell to approximate this lognormal distribution under accumulation conditions. Each of these classes acts autonomously in the sense of melting, refreezing and sublimating. A scheme of the snow cover is illustrated in Fig. 2. The snow water equivalent (S_{SWE_t}) of a given day t per class is calculated by Eq. (1) where P_{R_t} and P_{S_t} are fluid and solid precipitation in mm, respectively, M_t is snow melt and E_{S_t} is sublimation of snow. All variables are given in mm SWE.

$$S_{\mathrm{SWE}_t} = S_{\mathrm{SWE}_{t-1}} + P_{\mathrm{R}_t} + P_{\mathrm{S}_t} - M_t - E_{\mathrm{S}_t} \tag{1}$$

Snow melt is calculated by a temperature index approach (see for example Hock, 2003). Equation (2) is used:

$$M_t = \min(S_{\mathrm{SWE}_t}; P_{\mathrm{R}_t} \cdot \varepsilon \cdot T_{\mathrm{AIR}} + D_{\mathrm{f}_t} \cdot T_{\mathrm{AIR}}) \tag{2}$$

where M_t is snow melt in mm, ε is the quotient of specific heat of water and melting energy, T_{AIR} is the air temperature in °C and D_{f_t} [mm °C^{-1}] is the snow melt factor of

HESSD
12, 609–637, 2015

A conceptual, distributed snow redistribution model

S. Frey and H. Holzmann

a given day t estimated by Eq. (3):

$$D_{f_t} = \left(-\cos\left(J\cdot\frac{2\pi}{365}\right)\cdot\frac{D_U - D_L}{2} + \frac{D_U - D_L}{2}\right)\cdot M_{RED_t} \tag{3}$$

with

$$M_{RED_t} = \begin{cases} D_{RED}, & S_{fresh} \geq S_{CRIT} \\ M_{RED_{t-1}} + \dfrac{(1 - D_{RED_{t-1}})}{5}, & S_{fresh} < S_{CRIT} \end{cases} \tag{4}$$

where J is the Julian day of the year, D_U and D_L are the upper and lower boundaries of D_f, respectively, and M_{RED} is a reduction factor to account for the higher albedo caused by freshly fallen snow calculated by Eq. (4). S_{CRIT} is the critical snow depth of fresh snow in mm necessary to increase the albedo, whereas S_{fresh} is the actual snow depth of fresh snow in mm. For fresh snow depth larger than S_{CRIT}, D_f is lowered to a reduced melting factor D_{RED}.

For the estimation of snow sublimation, Eq. (5) is used, where E_{SP} refers to potential sublimation of snow in mm, E_P is the potential evapotranspiration in mm and E_R is a correction factor to reduce E_P.

$$E_{SP_t} = E_{P_t}\cdot E_R \tag{5}$$

The snow cover in COSERO is treated as porous medium and therefore is able to store a certain amount of liquid water (S_l) in dependency of the snow pack density (ρ) calculated using Eq. (6).

$$S_{l_t} = (S_{SWE_t} - S_{l_{t-1}})\cdot(S_{lMAX} - (\rho - \rho_{MAX})\cdot S_{l\rho}) \tag{6}$$

Where S_{lMAX} is the maximum water holding capacity at the maximum snow density of the snow pack ρ_{MAX} [g cm^{-3}] and $S_{l\rho}$ describes the decrease of water holding capacity with increasing snow density ρ in cm^3 g^{-1}.

HESSD
12, 609–637, 2015

At negative air temperatures, retained melt water has the ability to refreeze in the snow pack. The potential amount of refrozen water (S_R) is estimated by Eq. (7), where R_f is the refreezing factor. As long as there is enough fluid water in the snow pack, actual refreezing will be equal to potential refreezing.

$$S_R = R_f \cdot (T_{AIR} \cdot (-1)) \tag{7}$$

Refrozen water is treated in the same way as snow. The amount of water leaving the snow cover then equals snowmelt minus retained water.

Snow density (ρ) of each class is calculated using a sigmoid function shown in Eqs. (8) and (9) where ρ_{max} and ρ_{min} are the respective maximum and minimum values of ρ, T_{AIR} is the temperature of the air mass above the snow layer and ρ_{scale} and T_{scale} are scaling coefficients to calculate a transition temperature (T_{tr}) for the estimation of the snow density. Herby, ρ_{scale} adjusts the slope of the function, whereas T_{scale} is responsible for a shift on the x axis. These two parameters are set to fixed values of 1.2 and 1, respectively. The solution of Eqs. (8) and (9) is illustrated in Fig. 3 for a range of typical air temperatures, where snowfall occurs. Already fallen snow can reach a higher density then fresh snow. Its density is calculated using a settling constant until the maximum density is reached. This settling is only dependent on time.

$$\rho = (\rho_{MAX} - \rho_{MIN}) \cdot \left(\frac{T_{tr}}{\sqrt{1 + (T_{tr})^2}} + 1 \right) \cdot 0.5 + \rho_{MIN} \tag{8}$$

with

$$T_{tr} = \frac{T_{AIR}}{\rho_{scale}} + T_{scale} \tag{9}$$

The COSERO model considers both snow and glacier ice melt processes. Ice melt (M_{ICE}) is computed by means of a day degree method (see Eq. 10) and uses separate

HESSD
12, 609–637, 2015

parameter sets. Here, D_{ICE} refers to the ice melt factor in mm °C^{-1}. A prerequisite of ice melt is the full depletion of the overlying snow cover. Spatial information of glaciers are taken from the Randolph Glacier Inventory version 3.2 (Arendt et al., 2012).

$$M_{ICE} = D_{ICE} \cdot T_{AIR} \tag{10}$$

3.2 Snow transport model

The model redistributes snow only to grid cells providing the steepest slope (acceptor cell) in the direct neighbourhood of the raster cell it searches from (donor cell). If more than one cell shows the same (largest) difference in elevation, the amount of donated snow is distributed equally to the number of acceptor cells. The actual amount of snow being redistributed depends on the steepness of the slope, the age of the snow cover, considered by the density of snow, the type of land cover of the donor cell and the snow depth on the donor cell. The drier (lighter, less dense) the snow cover the higher the portion which is available for the redistribution routine (Eq. 12). The maximum density of snow, which is to be set as a model parameter and has the standard value of 0.45 g cm^{-3}, acts as a threshold where snow is unable to be moved. The availability of snow for transport is determined by a vegetation-based threshold value (H_v) for each class of land cover. This value can also be interpreted as a roughness coefficient for areas, where no or hardly any vegetation is present like in alpine and nival elevations. If the snow depth (S [mm]) of a raster cell exceeds H_v [mm], snow transport from that cell is activated and redistribution is calculated by solving Eqs. (11) and (12).

$$S_{SWE_A} = \max(S_D - H_v; 0) \cdot f_\rho \cdot \frac{1}{\sum A} \cdot C \tag{11}$$

With

$$f_\rho = \left(\frac{(\rho_{MAX} - \rho_D)}{\rho_{MAX}} \cdot e^{\left(-\frac{\rho_D}{\rho_{MAX}}\right)} \right) \cdot \frac{\alpha}{90} \tag{12}$$

HESSD
12, 609–637, 2015

Where S_{SWE} is the amount of snow water equivalent that is redistributed from the donor cell (D) to the available acceptor cell(s) (A), ρ_{D} is the density of snow on the donor cell, ρ_{MAX} is the possible maximum density of snow, α is the angle of the slope between the donor and acceptor cells in degree and C is a correction coefficient that can be calibrated.

Figure 4 illustrates the shape of the distribution coefficient f_p as a function of different elevation gradients between the acceptor and donor cells and of the snow density. On acceptor cells redistributed snow is treated as fresh snow in the sense, that it is distributed to the snow classes according to the log-normal distribution.

4 Case study in the catchment the Ötztaler Ache, Tyrol, Austria

4.1 Catchment description

The catchment of Ötztaler Ache at gauge Huben, situated in western Austria at the Italian border, covers an area of 511 km^2 and has an altitudinal range between 1185 m a.s.l. at the gauge at Huben and 3770 m a.s.l. at its highest peaks. Due to the use of a 1 km × 1 km gridded DEM, the highest grid cell has a mean elevation of 3450 m a.s.l., whereas the lowest cell has an elevation of 1250 m a.s.l. (Fig. 5). About 30 % of its area is covered by vegetation, mainly pastures and meadows. Glaciers cover about 19 % leading to an annual ice melt contribution of about 25 % of the total runoff at Huben, while 41 % of the discharge has its origin in snowmelt (Weber et al., 2010). Table 1 gives an overview of the land cover.

4.2 Input data

Gridded meteorological data of precipitation and air temperature are required to run the model. These data are provided by the INCA dataset (Haiden et al., 2011) allowing a direct use in the model without the need for pre-processing. INCA data are available since 2003. However, in 2003 and 2004, they are afflicted with errors. Therefore, these

HESSD
12, 609–637, 2015

years have been used as a warm-up period for the model. Six land use classes were derived from the most recent CORINE data set (CLC2006 version 17, see EEA, 1995). These classes and their fractures in the catchment of Ötztaler Ache are given by Table 1. It should be pointed out, that neither radiation nor wind speed or wind directory data are necessary to run the model.

4.3 Model calibration

The hydrological model was calibrated during the period from 2005 to 2008 using a Rosenbrock's automated optimization routine (Rosenbrock, 1963). Target of the calibration was a good fit of runoff using the Kling–Gupta-Model-Efficiency (Kling and Gupta, 2009; Kling et al., 2012) as objective function. Validation period was in the years 2009 and 2010. Both calibration and validation have been done with and without using the snow drift module. In the following model A refers to the model using snow transport, whereas model B stands for the classic model. Vegetation threshold values for snow detention were taken from previous studies (Liston and Sturm, 1998; Prasad et al., 2001). These are given by Table 1. For evaluation, besides runoff in the validation period, snow cover data from MODIS (8 day maximum snow cover, version 5) satellite images (Hall et al., 2002) were used to compare the performance of both models.

5 Results

5.1 Discharge

Figure 6 shows a comparison of total discharge using model A and B at the gauge Huben for the year 2006. Both models result in similar quality criteria in the calibration as well as in the validation period (see Table 2). Maximum differences in the mean daily discharges between the two models reach up to 12.1 $m^3 s^{-1}$ leading to a relative difference of minus 9 up to 44 % of model A in respect to model B. In total, model A generates about 300 mm more discharge in five years than model B (Fig. 7).

HESSD
12, 609–637, 2015

5.2 Spatially distributed snow cover data

Figure 8 compares model A and B with MODIS data. Both the accumulation period in winter and the ablation period in spring and summer are represented well by both models. So are cold periods in summer, where the snow line descents and therefore larger parts in the catchment are covered by a snow layer, meaning that only little effect of the transport model can be noticed comparing model A and B with MODIS data and both models show similar model efficiencies (Table 2).

5.3 Snow accumulation

The main reason for developing a snow transport model was the prevention of "snow towers" – accumulation of snow over several years in high mountainous regions. Figure 9 presents model behaviour of model A and B with respect to the accumulation of snow in elevations above 2800 m a.s.l. This elevation was chosen because here none of the models indicates snow accumulation for more than one year and therefore snow accumulation in lower altitudes is no problem. After seven years of modelling, model B shows snow depths of approx. 2900 mm SWE in elevations above 3400 m a.s.l. whereas model A does hardly show any accumulation behaviour in these altitudes. Note that in Fig. 9 only model results from 2005 to 2010 are shown while the warm-up period is missing due to a better perceptibility. Therefore snow depth does not start at zero in the figure while it does at the beginning of the modelling. Spatially distributed net loss and gain of snow for all raster cells in the watershed are presented in Fig. 10.

6 Discussion

6.1 Discharge

In spring, at the beginning of the melting season, higher runoff is generated by model A due to a larger amount of snow in lower altitudes (see Fig. 7). Later in the year enhanced glacier melt is mainly responsible for higher discharge rates. About 200 mm have their origin in enhanced snowmelt, while the remaining 100 mm originate in amplified melt of glaciers. Assigned to the glaciated area in the basin, this leads to an additional loss of 500 mm of glaciers. The reason for this is transport of snow in warmer altitudes and therefore no or less remaining snow in the catchment. This leads to earlier and more snow free glacier surfaces producing more runoff due to glacier melt (see Fig. 7) and explains the peak in July and August in runoff difference.

6.2 Spatially distributed snow cover data

In Fig. 8 only little differences between model A and B can be distinguished. Reasons for this lay in the threshold due to vegetation and roughness of the surface. Satellite based snow cover information by MODIS are binary and so is the model output for comparing these results. Even if snow is transported to other cells, a residual of snow remains on the donor cell. In a binary system, no difference can be distinguished between cells holding much or little snow.

6.3 Snow accumulation

While using model B, the higher the elevation the more snow is situated on. However, model A shows less pronounces and in some time periods even contrary behaviour in the upper altitudes (see Fig. 9). This is a result of the slope dependency of the distribution model that transports more snow on greater slopes. Since mountains, in general, are steeper at their peaks and more shallow in the lower parts, snow will preferably be transported from the peak cell over a steep slope to the adjacent cell which normally has a moderate slope to its downward neighbour. This does reflect snow accumulations that can be observed in nature where peaks might be nearly snow free in spring while in shallower parts are still covered by a snow layer. While the raster cells covering peak regions act as donators only those cells located on slopes may receive and distribute snow at the same time (Fig. 10). Valley regions only receive snow. However, due to the

HESSD
12, 609–637, 2015

binary nature of MODIS data, the spatial snow depth distribution cannot be validated with observed satellite based data.

The impact of transported snow decreases with increasing catchment area when larger parts of the catchment are on low elevations where snow accumulation does not play an important role for modelling discharge. If focussing on the catchment of river Inn at gauge Oberaudorf, which covers an area of about 10 000 km^2, in five years about 15 mm SWE remain in the catchment due to snow accumulation processes instead of 300 mm in the Ötztal. These information are with respect to the total catchment area.

7 Conclusions

A model for redistribution of snow on a coarse 1 km × 1 km raster has been developed and tested in the catchment of Ötztaler Ache, Austria. While only little improvement of snow cover compared to MODIS data could be achieved, appearance of "snow towers" in high altitudes could be prevented. In terms of discharge at the outlet of the basin, both models show good results. However, the efficiency of model A (KGE) could be improved by 0.05 in the calibration and by 0.02 in the validation period. With respect to the entire watershed area the model using snow redistribution generates about 200 mm more runoff originated from snowmelt in five years than without considering this process. This does not only affect the water balance of the catchment but also amplifies glacier melt about 500 mm in five years, with respect to glaciated areas, due to longer time periods where glacier surfaces are fully snow free.

The integration of a snow transport module promotes the demand, that models work "right for the right reasons" and is an attempt to integrate more real process understanding into the model approach. Further work needs to be carried out with respect to validation of spatially distributed snow patterns. For this purpose, satellite images from Landsat might be of use providing a higher spatial resolution than MODIS.

HESSD
12, 609–637, 2015

Acknowledgements. The authors thank their colleagues for continuing support and discussion around the coffee breaks. Special thanks to Herbert Formayer and David Leidinger of the institute of meteorology, BOKU, for supplying the INCA data.

References

Arendt, A., Bolch, T., Cogley, J. G., Gardner, A., Hagen, J.-O., Hock, R., Kaser, G., Pfeffer, W. T., Moholdt, G., Paul, F., Radić, V., Andreassen, L., Bajracharya, S., Barrand, N., Beedle, M., Berthier, E., Bhambri, R., Bliss, A., Brown, I., Burgess, D., Burgess, E., Cawkwell, F., Chinn, T., Copland, L., Davies, B., De Angelis, H., Dolgova, E., Filbert, K., Forester, R. R., Fountain, A., Frey, H., Giffen, B., Glasser, N., Gurney, S., Hagg, W., D., H., Haritashya, U. K., Hartmann, G., Helm, C., Herreid, S., Howat, I., Kapusti, G. G., Khromova, T., Kienholz, C., Köonig, M., Kohler, J., Kriegel, D., Kutuzov, S., Lavrentiev, I., Le Bris, R., Lund, J., Manley, W., Mayer, C., Miles, E., Li, X., Menounos, B., Mercer, A., Mölg, N., Mool, P., Nosenko, G., Negrete, A., Nuth, C., Pettersson, R., Racoviteanu, A., Ranzi, R., Rastner, P., Rau, F., Raup, B., Rich, J., Rott, H., Schneider, C., Seliverstov, Y., Sharp, M., Siguosson, O., Stokes, C., Wheate, R., Winsvold, S., Wolken, G., Wyatt, F., and Zheltyhina, N.: Randolph Glacier Inventory – A Dataset of Global Outliners: Version 3.2, Digital Media, Boulder, CO, USA, 2012.

Barros, A. P. and Lettenmaier, D. P.: Dynamic modeling of orographically induced precipitation, Rev. Geophys., 32, 265–284, doi:10.1029/94RG00625, 1994.

Bartelt, P. and Lehning, M.: A physical SNOWPACK model for the Swiss avalanche warning: Part I: Numerical model, Cold Reg. Sci. Technol., 35, 123–145, doi:10.1016/S0165-232X(02)00074-5, 2002.

Bergström, S.: Development and Application of a Conceptual Runoff Model for Scandinavian Catchments, SMHI Reports RHO, No. 7, Norrköping, 1976.

Bernhardt, M., Zängl, G., Liston, G. E., Strasser, U., and Mauser, W.: Using wind fields from a high-resolution atmospheric model for simulating snow dynamics in mountainous terrain, Hydrol. Process., 23, 1064–1075, doi:10.1002/hyp.7208, 2009.

Bernhardt, M., Liston, G. E., Strasser, U., Zängl, G., and Schulz, K.: High resolution modelling of snow transport in complex terrain using downscaled MM5 wind fields, The Cryosphere, 4, 99–113, doi:10.5194/tc-4-99-2010, 2010.

HESSD

12, 609–637, 2015

Bøggild, C. E., Knudby, C. J., Knudsen, M. B., and Starzer, W.: Snowmelt and runoff modelling of an Arctic hydrological basin in west Greenland, Hydrol. Process., 13, 1989–2002, doi:10.1002/(SICI)1099-1085(199909)13:12/13<1989::AID-HYP848>3.0.CO;2-Y, 1999.

Donald, J. R., Soulis, E. D., Kouwen, N., and Pietroniro, A.: A land cover-based snow cover representation for distributed hydrologic models, Water Resour. Res., 31, 995–1009, doi:10.1029/94WR02973, 1995.

EEA: CORINE Land Cover Project, available at: http://www.eea.europa.eu/publications/COR0-landcover (last access: 15 November 2014), 1995.

Essery, R., Li, L., and Pomeroy, J.: A distributed model of blowing snow over complex terrain, Hydrol. Process., 13, 2423–2438, doi:10.1002/(SICI)1099-1085(199910)13:14/15<2423::AID-HYP853>3.0.CO;2-U, 1999.

Garvelmann, J., Pohl, S., and Weiler, M.: From observation to the quantification of snow processes with a time-lapse camera network, Hydrol. Earth Syst. Sci., 17, 1415–1429, doi:10.5194/hess-17-1415-2013, 2013.

Haiden, T., Kann, A., Wittmann, C., Pistotnik, G., Bica, B., and Gruber, C.: The Integrated Nowcasting through Comprehensive Analysis (INCA) system and its validation over the eastern Alpine region, Weather Forecast., 26, 166–183, doi:10.1175/2010WAF2222451.1, 2011.

Hall, D. K., Riggs, G. A., Salomonson, V. V, DiGirolamo, N. E., and Bayr, K. J.: MODIS snow-cover products, Remote Sens. Environ., 83, 181–194, doi:10.1016/S0034-4257(02)00095-0, 2002.

Helfricht, K., Schöber, J., Schneider, K., Sailer, R., and Kuhn, M.: Interannual persistence of the seasonal snow cover in a glacierized catchment, J. Glaciol., 60, 889–904, doi:10.3189/2014JoG13J197, 2014.

Herrnegger, M., Nachtnebel, H.-P., and Haiden, T.: Evapotranspiration in high alpine catchments – an important part of the water balance!, Hydrol. Res., 43, 460–475, doi:10.2166/nh.2012.132, 2012.

Hock, R.: Temperature index melt modelling in mountain areas, J. Hydrol., 282, 104–115, doi:10.1016/S0022-1694(03)00257-9, 2003.

Kling, H. and Gupta, H.: On the development of regionalization relationships for lumped watershed models: the impact of ignoring sub-basin scale variability, J. Hydrol., 373, 337–351, doi:10.1016/j.jhydrol.2009.04.031, 2009.

Kling, H., Fuchs, M., and Paulin, M.: Runoff conditions in the upper Danube basin under an ensemble of climate change scenarios, J. Hydrol., 424–425, 264–277, doi:10.1016/j.jhydrol.2012.01.011, 2012.

Kling, H., Stanzel, P., Fuchs, M., and Nachtnebel, H.-P.: Performance of the COSERO precipitation-runoff model under non-stationary conditions in basins with different climates, Hydrol. Sci. J., online first, doi:10.1080/02626667.2014.959956, 2014a.

Kling, H., Stanzel, P., and Preishuber, M.: Impact modelling of water resources development and climate scenarios on Zambezi River discharge, J. Hydrol. Reg. Stud., 1, 17–43, doi:10.1016/j.ejrh.2014.05.002, 2014b.

Liston, G. E.: Representing subgrid snow cover heterogeneities in regional and global models, J. Climate, 17, 1381–1397, doi:10.1175/1520-0442(2004)017<1381:RSSCHI>2.0.CO;2, 2004.

Liston, G. and Sturm, M.: A snow-transport model for complex terrain, J. Glaciol., 44, 498–516, 1998.

Moore, R. J.: The PDM rainfall-runoff model, Hydrol. Earth Syst. Sci., 11, 483–499, doi:10.5194/hess-11-483-2007, 2007.

Nachtnebel, H. P., Baumung, S., and Lettl, W.: Abflussprognosemodell für das Einzugsgebiet der Enns und Steyer, Institute of Water Management, Hydrology and Hydraulic Engineering, University of Natural Resources and Applied Life Sciences, Vienna, Austria, 1993 (in German).

Nikulin, G., Kjellström, E., Hansson, U., Strandberg, G., and Ullerstig, A.: Evaluation and future projections of temperature, precipitation and wind extremes over Europe in an ensemble of regional climate simulations, Tellus A, 63, 41–55, doi:10.1111/j.1600-0870.2010.00466.x, 2011.

Pohl, S., Garvelmann, J., Wawerla, J., and Weiler, M.: Potential of a low-cost sensor network to understand the spatial and temporal dynamics of a mountain snow cover, Water Resour. Res., 50, 2533–2550, doi:10.1002/2013WR014594, 2014.

Pomeroy, J. W., Gray, D. M., Shook, K. R., Toth, B., Essery, R. L. H., Pietroniro, A., and Hedstrom, N.: An evaluation of snow accumulation and ablation processes for land surface modelling, Hydrol. Process., 12, 2339–2367, doi:10.1002/(SICI)1099-1085(199812)12:15<2339::AID-HYP800>3.0.CO;2-L, 1998.

Pomeroy, J. W., Gray, D. M., Hedstrom, N. R., and Janowicz, J. R.: Prediction of seasonal snow accumulation in cold climate forests, Hydrol. Process., 16, 3543–3558, doi:10.1002/hyp.1228, 2002.

Prasad, R., Tarboton, D. G., Liston, G. E., Luce, C. H., and Seyfried, M. S.: Testing a blowing snow model against distributed snow measurements at Upper Sheep Creek, Idaho, United States of America, Water Resour. Res., 37, 1341–1356, doi:10.1029/2000WR900317, 2001.

Rechenraum: Der oe3d Datensatz, available at: www.oe3d.at (last access: 18 November 2014), 2014.

Rosenbrock, H. H.: Some general implicit processes for the numerical solution of differential equations, Comput. J., 5, 329–330, doi:10.1093/comjnl/5.4.329, 1963.

Schaefli, B., Hingray, B., Niggli, M., and Musy, A.: A conceptual glacio-hydrological model for high mountainous catchments, Hydrol. Earth Syst. Sci., 9, 95–109, doi:10.5194/hess-9-95-2005, 2005.

Shulski, M. D. and Seeley, M. W.: Application of snowfall and wind statistics to snow transport modeling for snowdrift control in minnesota, J. Appl. Meteorol., 43, 1711–1721, doi:10.1175/JAM2140.1, 2004.

Stanzel, P. and Nachtnebel, H. P.: Mögliche Auswirkungen des Klimawandels auf den Wasserhaushalt und die Wasserkraftnutzung in Österreich (in German), Oesterr. Wasser- Abfallwirtsch., 62, 180–187, doi:10.1007/s00506-010-0234-x, 2010.

Stanzel, P., Kahl, B., Haberl, U., Herrnegger, M., and Nachtnebel, H. P.: Continuous hydrological modelling in the context of real time flood forecasting in alpine Danube tributary catchments, IOP C. Ser. Earth Env., 4, 012005, doi:10.1088/1755-1307/4/1/012005, 2008.

Thornthwaite, C. W.: An approach toward a rational classification of climate, Geogr. Rev., 38, 55–94, 1948.

Weber, M., Braun, L., Mauser, W., and Prasch, W.: Contribution of rain, snow- and icemelt in the upper Danube discharge today and in the future, Geogr. Fis. Din. Quat., 33, 221–230, 2010.

Winstral, A., Elder, K., and Davis, R. E.: Spatial snow modeling of wind-redistributed snow using terrain-based parameters, J. Hydrometeorol., 3, 524–538, doi:10.1175/1525-7541(2002)003<0524:SSMOWR>2.0.CO;2, 2002.

Wood, E. F., Lettenmaier, D. P., and Zartarian, V. G.: A land-surface hydrology parameterization with subgrid variability for general circulation models, J. Geophys. Res., 97, 2717–2728, doi:10.1029/91JD01786, 1992.

HESSD

12, 609–637, 2015

A conceptual, distributed snow redistribution model

S. Frey and H. Holzmann

Table 1. Land use classes used in COSERO (derived from CORINE land cover data) and their proportion in the Ötztal. Snow holding capacities H_v for each type of land use are taken from (Liston and Sturm, 1998; Prasad et al., 2001).

Land use class	proportion [%]	Snow holding capacity H_v
Build-up areas	1.2	100
Pastures and meadows	20.9	500
Coniferous forests	8.1	2500
Sparsely vegetated areas	20.9	300
Bare rocks	29.5	200
Glaciers	19.4	200

HESSD
12, 609–637, 2015

Table 2. Comparison of performances of model A and B with respect to snow cover and runoff. For snow cover coefficient of determination (R^2) was used, whereas Kling–Gupta-Efficiency (Kling and Gupta, 2009) was used for runoff. Note, that snow cover was not used as calibration criterion.

	Calibration		Validation	
	Snow cover (R^2)	Runoff (KGE)	Snow cover (R^2)	Runoff (KGE)
MODEL A	0.78	0.93	0.74	0.92
MODEL B	0.70	0.88	0.66	0.90

HESSD
12, 609–637, 2015

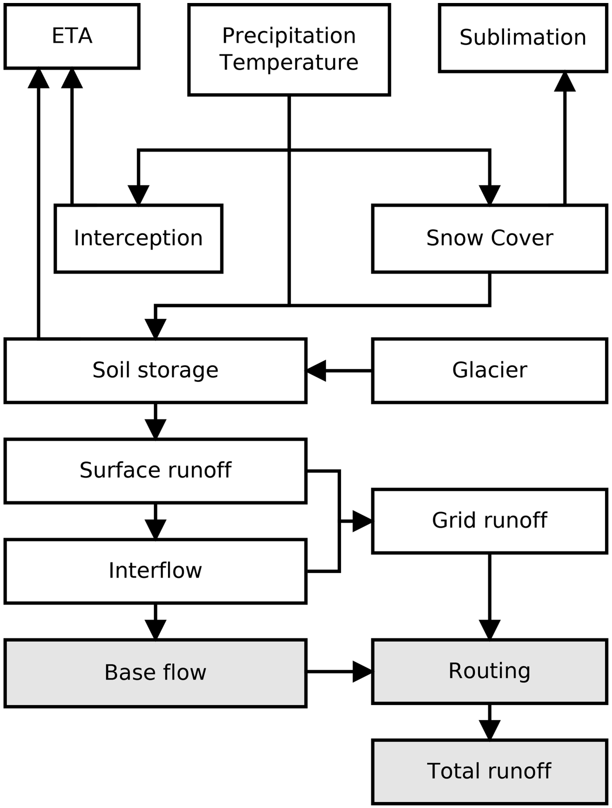

Figure 1. Flow chart of the conceptual model COSERO. Potential evapotranspiration is estimated using the Thornthwaite method (Thornthwaite, 1948). White parts represent distributed processes, greyish parts are calculated on a subbasin scale. Snow transport is implemented in the snow cover module.

HESSD
12, 609–637, 2015

A conceptual, distributed snow redistribution model

S. Frey and H. Holzmann

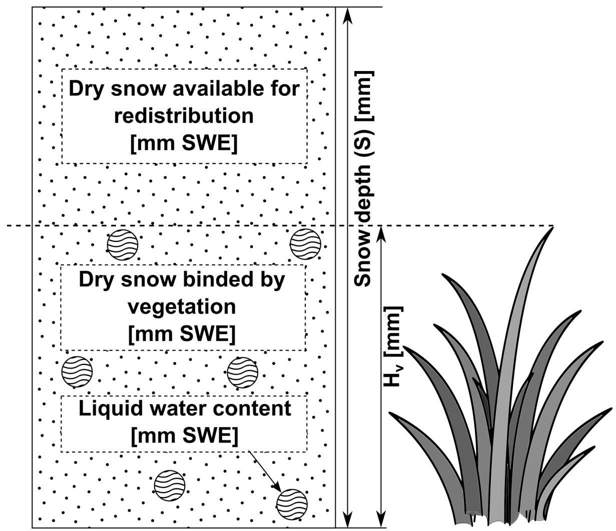

Figure 2. Schematic view of the snow cover in COSERO. Every cell consists of five snow classes of which each is composed in the way described but acts autonomously with respect to melting, refreezing, sublimating and redistribution.

HESSD
12, 609–637, 2015

A conceptual, distributed snow redistribution model

S. Frey and H. Holzmann

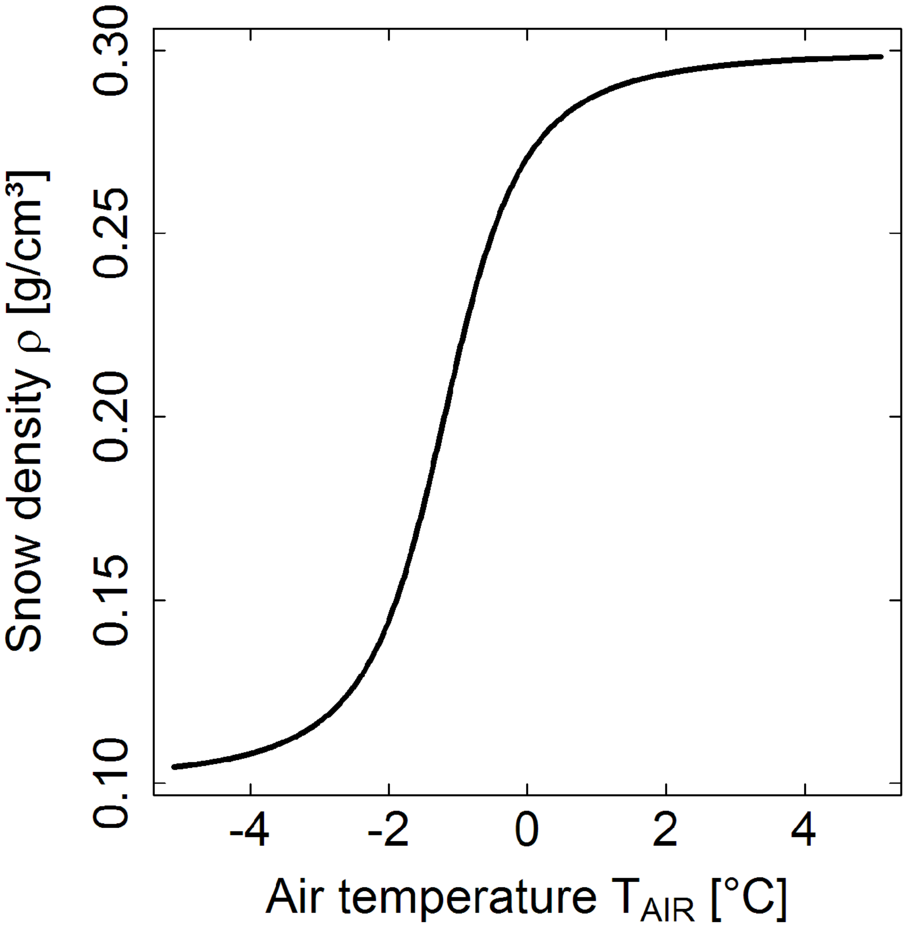

Figure 3. Estimation of the density of snow using Eqs. (8) and (9). Minimum and maximum densities of the snow cover are 0.1 and 0.3, respectively. Standard values for ρ_{scale} and T_{scale} are 1.2 and 1, respectively.

HESSD
12, 609–637, 2015

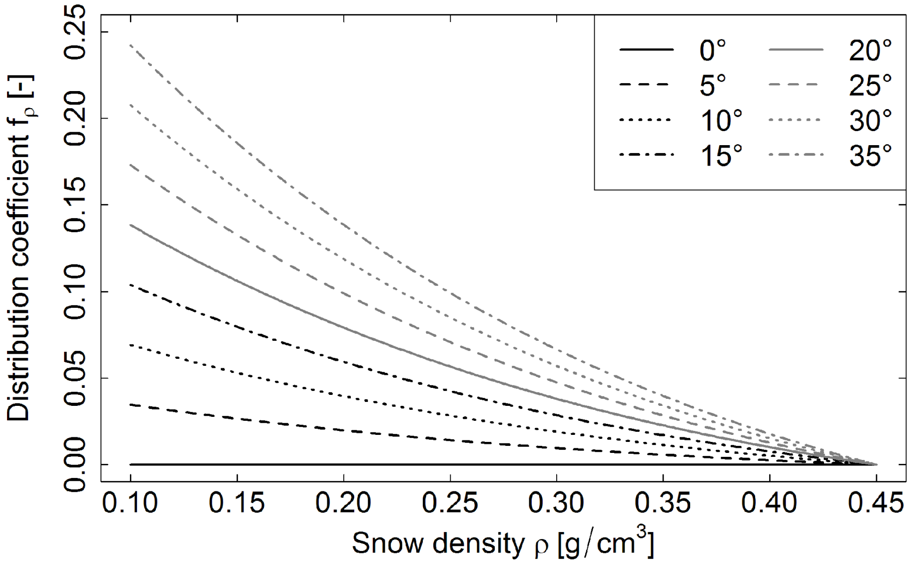

Figure 4. Shapes of the distribution coefficient in dependency of different slope angles and snow densities. When using an 1 km × 1 km raster, slopes greater than 35° hardly exist. If cold snow with a density of 0.1 is located on a slope of 35°, a portion of 25 % of the available snow is transported to the neighbour cell. If the snow density reaches its maximum value, no transport occurs regardless of the slope.

HESSD
12, 609–637, 2015
A conceptual, distributed snow redistribution model
S. Frey and H. Holzmann

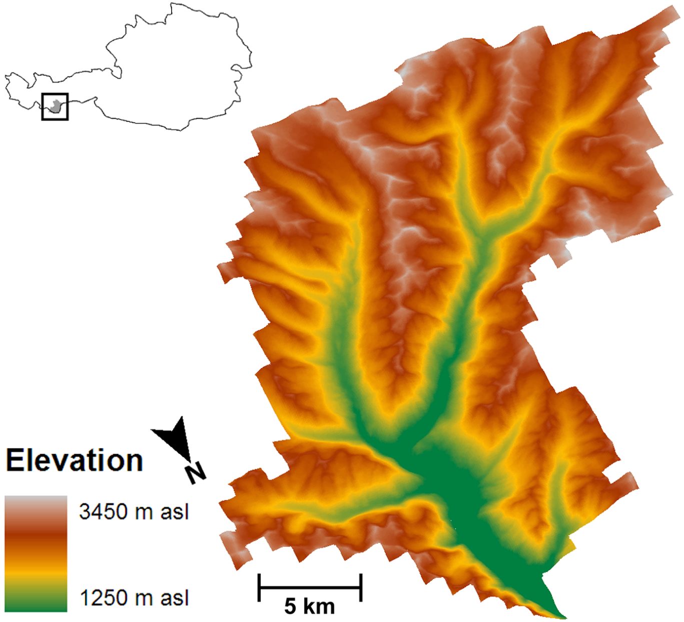

Figure 5. Elevation levels of the Ötztal using a 1 km × 1 km grid ranging from 1250 m at the outlet at Huben to 3450 m a.s.l. in the peak regions. For visualisation the free available oe3d DEM (Rechenraum, 2014) was used.

HESSD
12, 609–637, 2015

A conceptual, distributed snow redistribution model

S. Frey and H. Holzmann

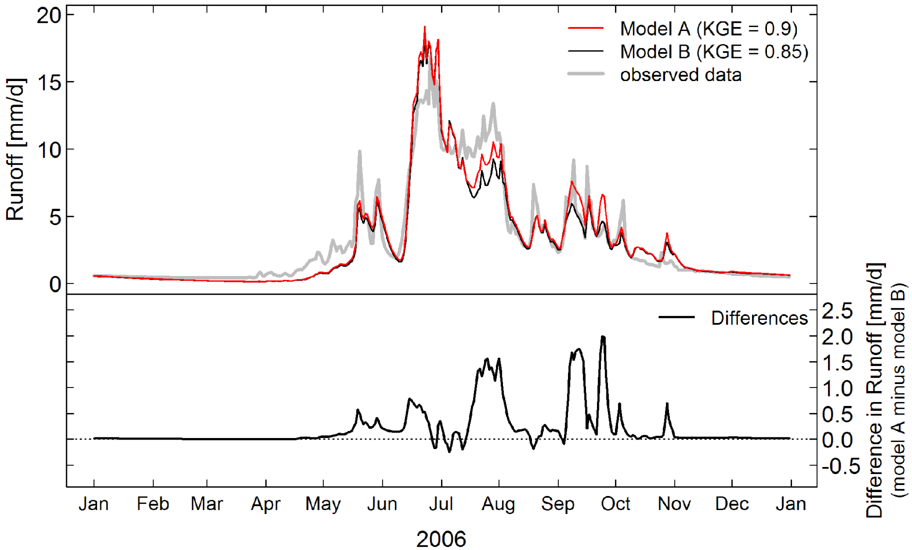

Figure 6. Specific runoff at the outlet at Huben is modelled with (model A) and without (model B) using the snow redistribution routine. In the early snow melt period, more runoff is generated by model A because snow accumulates rather in lower than in higher levels. In summer, enhanced glacier melt leads to more runoff by model A.

HESSD
12, 609–637, 2015

A conceptual, distributed snow redistribution model

S. Frey and H. Holzmann

Title Page
Abstract | Introduction
Conclusions | References
Tables | Figures
◀| |▶
◀ ▶
Back | Close
Full Screen / Esc
Printer-friendly Version
Interactive Discussion

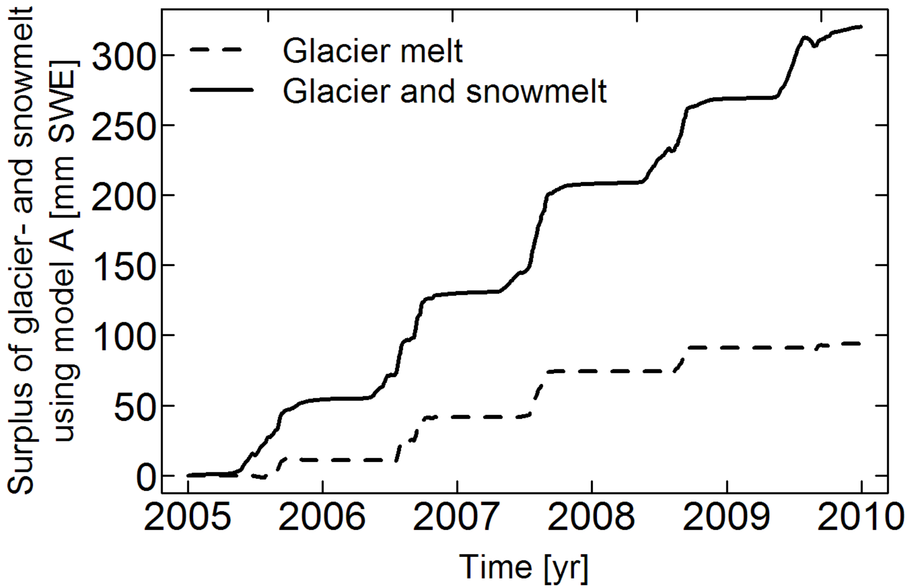

Figure 7. Accumulated differences (model A minus model B) in discharge at gauge Huben. Using model B, about 300 mm SWE in five years are remaining in the catchment due to snow accumulation processes and less glacier melt.

HESSD
12, 609–637, 2015

A conceptual, distributed snow redistribution model

S. Frey and H. Holzmann

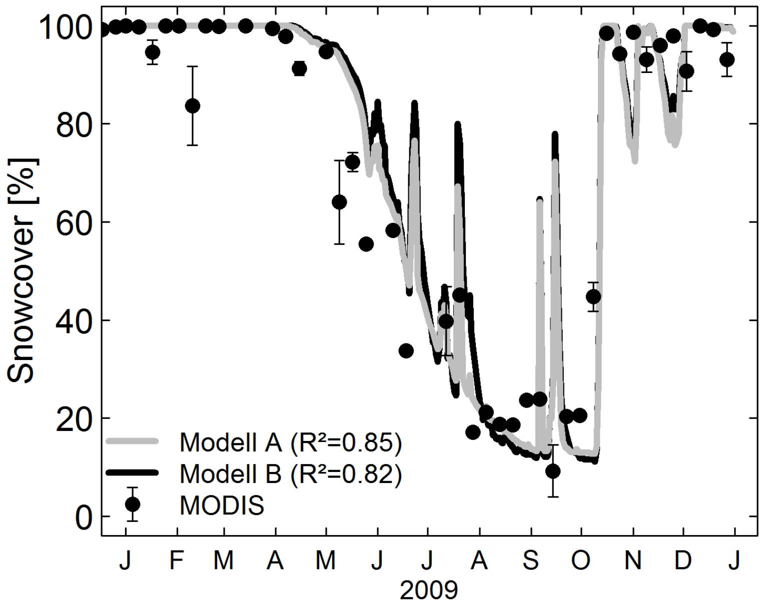

Figure 8. Snow cover in 2009 modelled by both model A and B compared with MODIS data. Reason of the little difference is the vegetation threshold. Even if snow is being transported, a residual of snow remains on the donor cell resulting in the cell marked as snow covered. Error bars refer to uncertainties due to cloud coverage.

HESSD
12, 609–637, 2015

A conceptual, distributed snow redistribution model

S. Frey and H. Holzmann

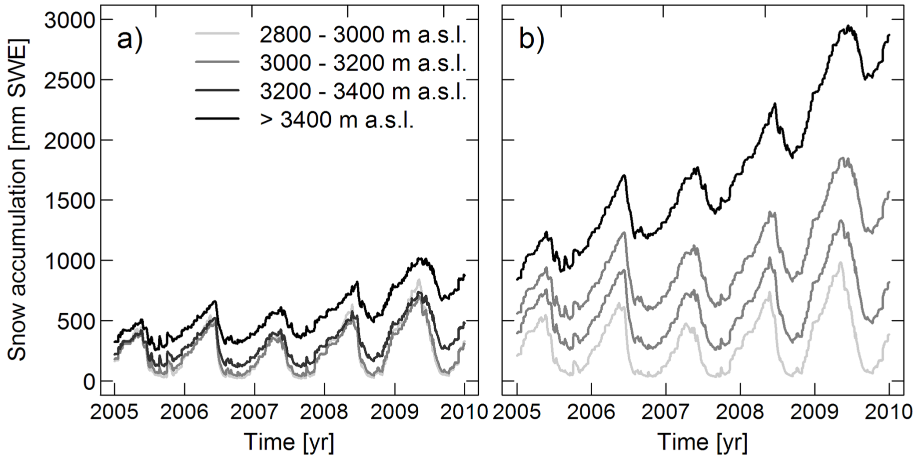

Figure 9. Behaviour of snow accumulation and melt of model A **(a)** and B **(b)** in the upper elevations. Model B leads to "snow towers" of approx. 2900 mm SWE in regions above 3400 m a.s.l. in seven years of modelling, whereas model A does not show such behaviour. On elevations lower 2800 m a.s.l. neither model A nor B show accumulation behaviour. Note that model results are shown from 2005 to 2010 without the warm-up period.

HESSD
12, 609–637, 2015

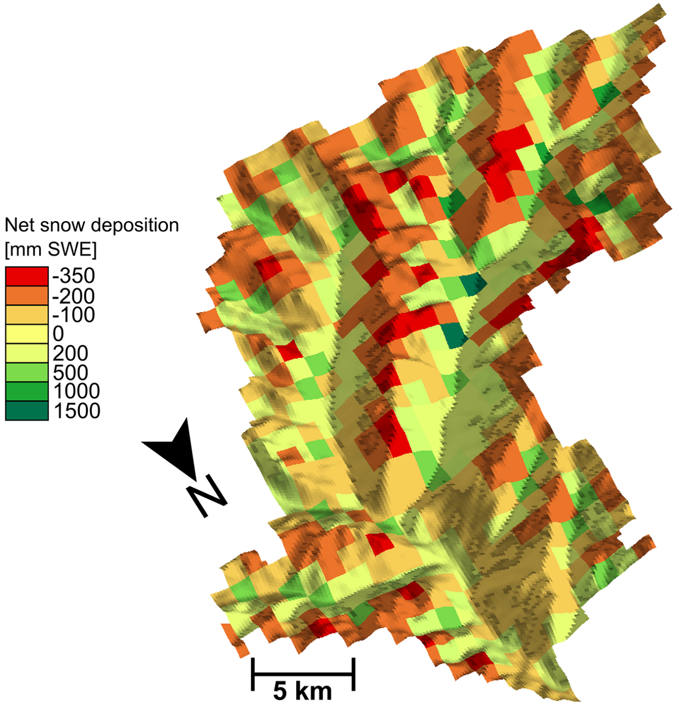

Figure 10. Net snow deposition in the catchment. Negative values refer to a net loss, positive to a net gain of snow. Raster cells in the peak regions act as donor cells and do not receive any snow whereas lower cells may act as donor and acceptor in the same time. For visualisation the free available oe3d DEM (Rechenraum, 2014) was used.

HESSD
12, 609–637, 2015

A conceptual, distributed snow redistribution model

S. Frey and H. Holzmann